Japanese Journal of Applied Physics

The Japan Society of Applied Physics

REGULAR PAPER

Effect of growing nanoparticle on the magnetic field induced filaments in a radio-frequency Ar/C_2H_2 discharge plasma

Japanese Journal of Applied Physics **59**, SHHC07 (2020) **REGULAR PAPER**
https://doi.org/**10.35848/1347-4065/ab78eb**

Effect of growing nanoparticle on the magnetic field induced filaments in a radio-frequency Ar/C_2H_2 discharge plasma

S. Jaiswal[1*], M. Menati[1], L. Couëdel[2], V. H. Holloman[3], V. Rangari[3], and E. Thomas Jr.[1]

[1]*Department of Physics, Auburn University, Auburn, AL 36849, United States of America*
[2]*Department of physics and engineering physics, University of Saskatchewan, Saskatoon, Saskatchewan S7N 5E2, Canada*
[3]*Department of Materials Science and engineering, Tuskegee University, Tuskegee, Alabama, United States of America*

[*]E-mail: surabhijaiswal73@gmail.com; szj0071@auburn.edu

Received November 5, 2019; revised February 5, 2020; accepted February 21, 2020; published online March 9, 2020

Growth of nanoparticles in plasmas is an emerging topic of research due to its numerous implications in industrial, and fusion plasmas applications. In this paper, effect of a magnetic field induced filaments on the growing nanoparticles and vice versa has been investigated. The experiment has been performed in a capacitive coupled radio-frequency Ar/C_2H_2 discharge. The magnetic field affect the plasma dynamics and confined it within the electrodes. At a very high magnetic field ($B \geqslant 1$ T) a stationary or moving filamentary structures are formed between the electrodes that are aligned along the magnetic field. These filamentary structures are found to be suppressed during nanoparticle growth. A particle in cell simulation has been performed to understand the suppression of these filamentary structure.

1. Introduction

The formation of dust particles in industrial plasma reactors is a topic of significant research interest. The presence of nanometer-to micrometer-sized particulates formed as a by-product of the etching process is unwanted because the dust particles can significantly change the electrical properties of the discharge and, subsequently lead to the pollution and contamination of the substrate. However, the dust particles can also be of value for technologies based on nanomaterials and nanocomposites, such as polymorphous silicon which is of interest for the manufacture of solar cells.[1)] In the laboratory, low pressure rf plasma discharges have been extensively used to produce good quality nanocrystals and nanopowders of broad range of materials.[2)] Therefore, the growth processes that lead to particle growth and, ultimately, achieving predictive control over those processes is of interest to many subfields of plasma physics.

Particle growth depends on the discharge parameters and, in turn, the appearance of the growing particles can significantly impact the properties of the surrounding plasma. Therefore, achieving better control over the discharge and plasma parameters can help control the particle growth process. One method to achieve this control is to apply a magnetic field to the plasma.

The presence of a magnetic field alters the transport properties of the electrons and ions in the plasma. And, at a sufficiently high magnetic field, the transport of the charged dust particles may also become affected. Therefore, in the presence of magnetic field the nanoparticle growth process and the morphology of growing nanoparticle is expected to be modified. A number of experiments have been reported on the growth process in weakly magnetized plasmas ($B \leqslant 0.1$ T).[3–5)] Here, the role of the magnetic field is to provide confinement to the electrons and ions and to provide some control over the plasma density. For example, in magnetron sputtering discharges,[4)] a dense metallic nanoparticles growth has been observed over the cathode. Also, is has been reported that the dust rotation arising from the ion $E \times B$ has been observed and used to enhance particle coating.[6)]

In this paper, we report on the formation of nanoparticles at high magnetic field and the coupling between the particle growth and the filamentation phenomenon. Specifically, it will be shown that in the formation of high density clouds of nanoparticles, the filamentation process can be suppressed.

Experiments are performed in the magnetized dusty plasma experiment (MDPX) device using a modified rf plasma source.[7)] Plasmas were generated in pure argon (Ar) or in a mixture of argon and acetylene (C_2H_2) gas. The magnetic field was varied from 0 to 2.0 T. The filaments appear in the plasma for magnetic fields $B \geqslant 0.5$ T. The growth of the nanoparticle will be shown to modify the discharge parameters and—after several growth cycles when the density of grown particles increased—lead to the suppression of the filaments. A numerical simulation has been performed to understand the effect of high density dust particles on the filaments.

The paper is organized as follows: in Sect. 2, we discuss the influence of a strong magnetic field on the plasma and the observations of plasma filaments. In Sect. 3, we describe the experimental arrangement in detail. In Sect. 4, we discuss the experimental results on the formation of nanoparticles and its effect on magnetic field induced filaments. Section 5 presents the results of a numerical simulation that investigates the effect of layer on the formation of filaments in a plasma. Finally, some brief concluding remarks are made in Sect. 6.

2. Plasma filamentation

In the attempt to study dusty plasmas at high magnetic fields in capacitively coupled plasmas, the formation of filaments was an unexpected phenomenon. The filaments appear in the plasma with or without the presence of the dust particles and have been reported in a variety of experiments.[8–11)] These filaments are structures that form along the magnetic field lines and appear as vertical columns, when viewed from the side, or as dots, rings, or spiral structures, when viewed from the top. Two views of filaments are shown in Fig. 1. Because the filaments are believed to be regions of either increased plasma density or possibly enhanced electron temperature, their presence disrupts the uniformity of the plasma, have an

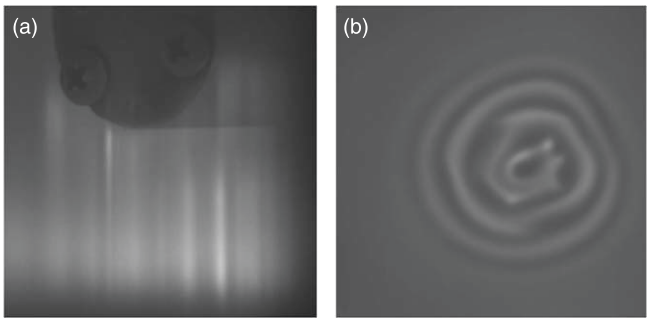

Fig. 1. View of filaments in the magnetized dusty plasma experiments (MDPX) device at Auburn University. (a) Side view of filaments near a dust shaker (object at the top right) in an argon plasma at $B = 1.76$ T. (b) Top view of filaments in an argon plasma at $B = 2.0$ T.

impact on the stability of the plasma and can act to perturb the behavior of dust particles in the plasma.

As discussed in the paper by Schwabe et al.[8] and in a recent paper by Thomas et al.[11] the filaments can be either stationary or mobile structures in the plasma. They often are observed to evolve on time scales of seconds; i.e. much longer than the typical μs to ms time scales associated with electron or ion dynamics in the plasma. As a result, in spite of the various observations of the filaments over the last decade, many of their properties remain poorly diagnosed. Furthermore, the vast time-scale differences between the electron and ion dynamics and the slow evolution of the filaments themselves has made both theoretical and computational studies of the filaments quite challenging.

Nonetheless, there has been some progress in understanding the interaction between the filaments and the dust particles. In their experiments on filamentation, Schwabe et al.[8] used dust particles as probes to investigate the behavior of the plasma. They noticed that for a relatively lower density of micro-particles, the change in the characteristics of the filamentation in the presence of dust particles was not notable. On the other hand, it was observed that covering one of the electrodes with a dielectric plate (glass) weakens the filamentation phenomenon and the conductivity of the boundaries can affect the phenomenon.

In another study by Couedel et al.[7] the effect of high magnetic field on growth process and morphology of the grown particles has been studied. They observed the formation of filaments started at magnetic fields of $B \geqslant 0.1$ T, which disturbed the whole process of particle growth. For the highest magnetic fields, $B \geqslant 2.5$ T, it became clear that the particle growth was significantly modified, but it remained unclear the extent of the coupling between the filaments and the particle growth. For this paper, clear evidence is presented on how the dust and the filaments are coupled.

3. Experimental arrangement

Experiments were performed using the MDPX facility. The MDPX device is a multi-user, high magnetic field experimental platform which consists of two main components: the superconducting magnet and a plasma chamber which can be changed according to the experimental requirements. The ability to vary the magnetic field in a well-controlled manner up to 3.5 T enables carefully controlled experiments over a wide range of magnetic field. The details of superconducting magnet of the MDPX device are described in previous articles.[12–14] For our experiment, the MDPX device was operated in its vertical configuration where the magnetic field lines were parallel to the gravity. The four superconducting coils were energized at the same current to produce a uniform magnetic field at the center of the experimental volume.

An ISO 100 (i.e. 100 mm flanges), six- way cross aluminum vacuum chamber consisting of parallel electrodes with a gap of 2.5 cm is used as a plasma source. The detailed description of the experimental setup is reported elsewhere.[7] A radio-frequency (13.56 MHz) plasma is formed between the electrodes at an rf power of 25 Watts in a background of argon gas. The disc shaped top electrode of diameter 50 cm was powered and surrounded by grounded ring [Fig. 2(a)]. The gap between the powered electrode and the ring were filled by using a ceramic cap for a better insulation. The bottom electrode of diameter 76.2 mm was kept on ground. A 1 mm × 25 mm × 75 mm notch was cut in the center of the bottom electrode to install the microcopy slides used for collecting the samples. The change in the discharge parameters during particle growth was monitored by measuring the change in the neutral pressure and self-bias voltage on the powered electrode.

The chamber was evacuated to a base pressure of 1 mTorr and then a combination of argon gas with a flow of 11.65 sccm and the acetylene flow of 2.3 sccm was injected into the chamber. The pressure was set to 500 mTorr by changing the pumping speed. Plasma was switched on for 90 s and then switched off. The grown nanoparticle cloud was illuminated using 532 nm laser of 100 mW power [See Fig. 2(b)] and the scattered light was recorded using a CCD camera with 30 fps.

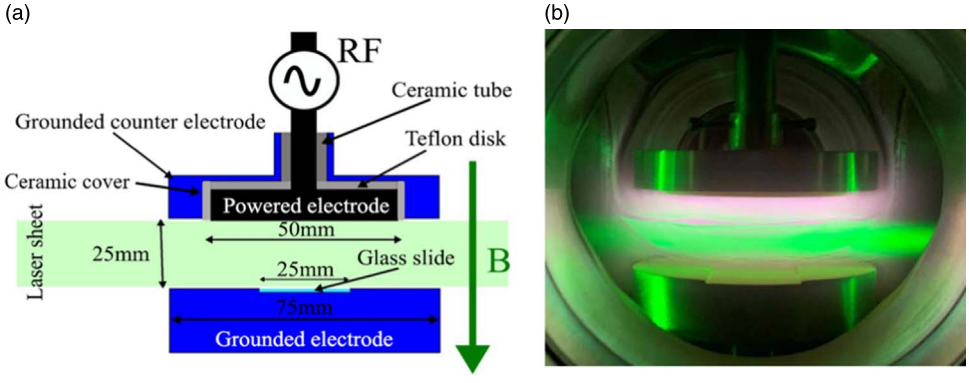

Fig. 2. (Color online) (a) Schematic of the electrode arrangement (b) snapshot of particle growth at no magnetic field.

This process was repeated for number of magnetic field settings.

4. Experimental results

First, we investigate the behavior of the plasma at different magnetic fields to illustrate the behavior of the filaments in the absence of the dust particles. Figure 3 shows the snapshots of the argon plasma glow at different magnetic fields. At zero magnetic field, shown in Fig. 3(a), the plasma glow has a generally uniform appearance and expands to fill much of the vacuum chamber volume between the top and bottom electrodes. With increasing magnetic field, the glow becomes localized beneath the top electrode. This suggest that the magnetic field has confined the radial transport of charged species in the plasma, i.e. the ions and electrons. The filaments begin to appear in the plasma above a magnetic field of 0.5 T.

Figure 3(b) shows a representative image of the plasma glow at $B = 1.5$ T. In this figure, the plasma is significantly compressed radially and is more localized to the region below the powered, top electrode. There is also the appearance of a vertical structures, aligned parallel to the magnetic field, that indicate the formation of the filamentary structures in the plasma. It is noted that there are two strong, stationary filaments that appeared just above the notches in the lower electrode; this will be a prominent feature throughout the remainder of this paper. It is noted that the filaments are moving throughout the electrode whereas the strong filaments at the notches locked at that location.

We next consider how the addition of grown nanoparticles impacts the plasma. Figure 4 shows the snapshots of scattered laser light from the growing nanoparticles. Without a magnetic field, the entire volume between electrodes becomes filled with nanoparticles as seen in Fig. 4(a). It is noted

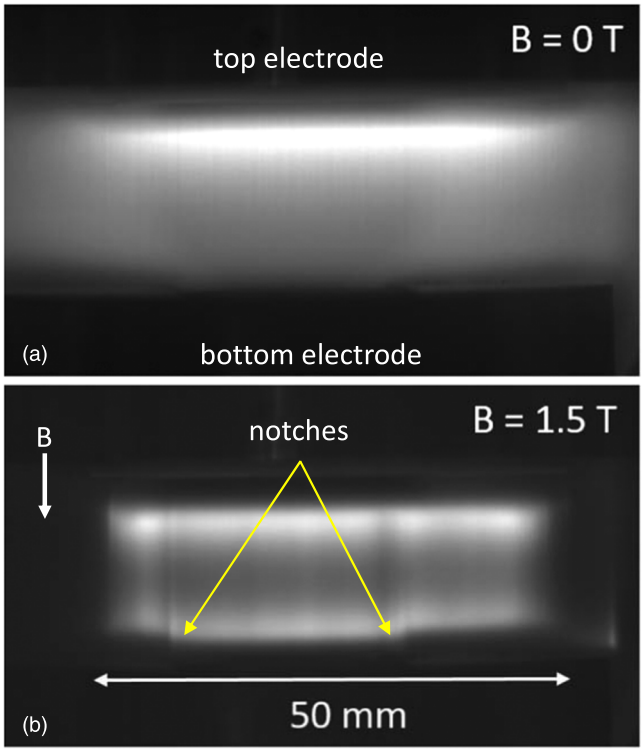

Fig. 3. (Color online) Snapshots of plasma glow (i.e. with no dust particles present) at (a) $B = 0$ T (b) at $B = 1.5$ T.

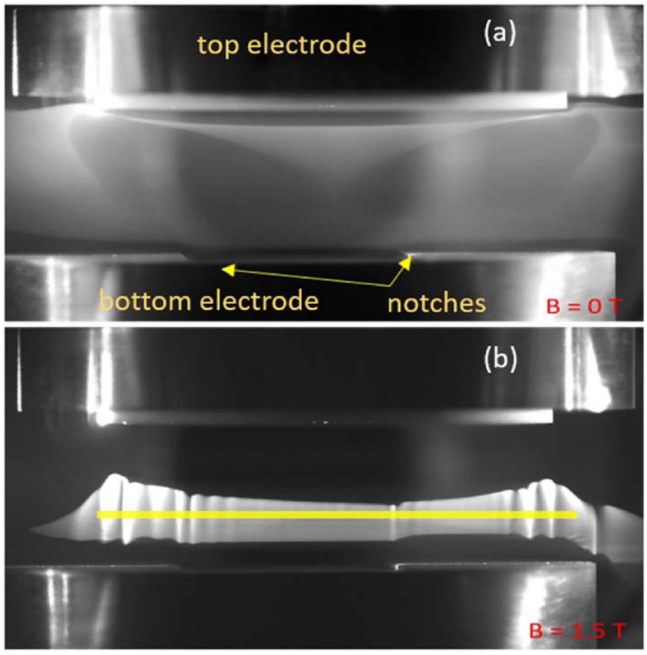

Fig. 4. (Color online) Images of the scattered laser light at different instants after discharge ignition for (a) $B = 0.0$ T, (b) $B = 1.5$ T. It is noted that the top and bottom electrodes are more clearly visible in this image. The yellow strip in (b) indicates the region that the space-time image used in Fig. 6.

that with the laser illumination, the location of the top and bottom electrodes becomes clearly visible as does the location of the notch in the lower electrode. At a high magnetic field of 1.5 T, the growing particles are confined in the sheath above the lower electrode as illustrated in Fig. 4(b). In addition, the filaments that formed between the electrodes appear to be correlated to regions of dense particle growth as can be seen from the localized regions of saturated light intensity.

To investigate the effect of nanoparticle growth in the plasma and magnetic field induced filaments a few changes were made to the experimental procedures that were originally described in Couëdel et al.[7] First, the flow rate of acetylene was increased slightly to allow a higher relative concentration of acetylene in the plasma. The pressure was set to 500 mTorr before plasma ignition using an Ar/C_2H_2 mixture ($Q_{Ar} = 11.65$ sccm and $Q_{C2H2} = 2.3$ sccm). Figure 5 shows the variation of the neutral pressure over the time duration of the plasma. It can be seen that after the discharge was turned on the pressure start decreasing. This indicates that, while the acetylene flow was kept constant, it was partially dissociated and lead to a nanoparticle growth.

The second change was the plasma discharge was operated with an extended duration of $t_{ON} = 300$ s as compared to a 60 s cycle in the earlier work. This had the effect of allowing multiple, sequential growth cycles of particles to occur in the plasma—leading to a substantially higher concentration of nanoparticles compared to previous work. This is illustrated in Fig. 6, which shows the space-time evolution of nanoparticle growth at a magnetic field of 2 T extracted from a 30 frame/second video recording of the particle growth process. In this figure, the horizontal axis is determined from the yellow strip that is shown in Fig. 4—approximately 65 mm wide 4 mm tall. This strip is then extracted from each image

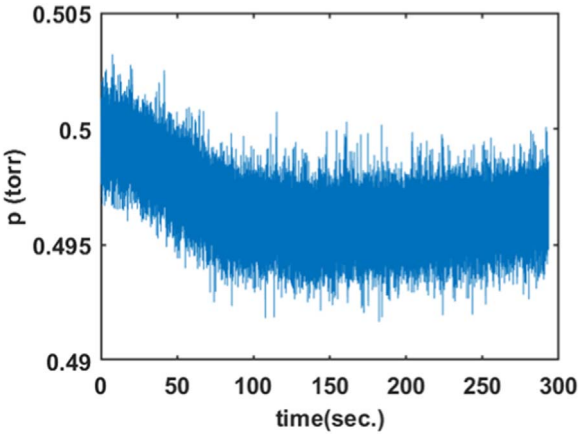

Fig. 5. (Color online) Pressure variation during the particle growth for $B = 2$ T.

of the video and stacked vertically to represent time. Time increases from the bottom of the image, going upward.

Several important features are observed in this image. First, the well-known cyclic growth behavior was observed as indicted by the "cycle" labels in the image. Each cycle has a period of particle growth (bright regions) followed by a black horizontal "gap" as the particles become large enough that they are no longer confined in the plasma. Additionally, there are several "fixed" vertical stripes are observed where fixed filamentary structures are appearing in the plasma. These are believed to be due to the notches and other perturbations on the top and bottom electrodes that cause current channels to be localized in the plasma.

However, the main feature that is reported in this paper is evolution of the filaments in the central region between the electrodes (indicated by the red stripe in Fig. 6. Due to strong magnetic field, there is a formation of mobile filaments that appear to disrupt the growth of the particles. These filaments were mostly observed during the first two growth cycles during the initial phases of particle growth. During Cycle 2 (at the outer edges of the plasma near $x = 15$ mm and $x = 45$ mm) and throughout Cycles 3–4, the appearance of the mobile filaments appears to become increasingly suppressed so that by Cycle 5, there is little evidence of filament formation.

5. Numerical simulation

To investigate if high density dust particles in the plasma could affect the formation of filaments, we have used a numerical simulation of the strongly magnetized plasma. As will be discussed later in this section, it is not possible to develop a simulation framework that can self-consistently model the complete time evolution of electron, ion, and dust dynamics—because of the widely different time scales associated with each plasma species. However, we have already achieved some success in using a numerical simulation to model the behavior of filaments in a strongly magnetized plasma.[15] The goal of these simulations is to add the influence of a dense dust layer—to be modeled as a dielectric surface that can absorb free electrons from the plasma—and to determine whether this layer can suppress the formation of the filaments.

In this simulation, the evolution of the plasma is determined by solving the plasma fluid equations along Poisson's equation. The effect of the increasing dust particle density will be modeled as a dielectric surface at the plasma boundary.

In this model we are assuming an isothermal plasma (constant electron and ion temperatures) at a density of $5 \times 10^{14}\,\mathrm{m}^{-3}$ in a rectangular plasma chamber. The set of equations considered in this model are the same as the set used by Park et al.[16]

$$\nabla^2\phi = -\frac{\rho}{\varepsilon}, \tag{1}$$

where ρ is the charge density and ε the electric permittivity that we have assumed to be constant throughout the plasmas

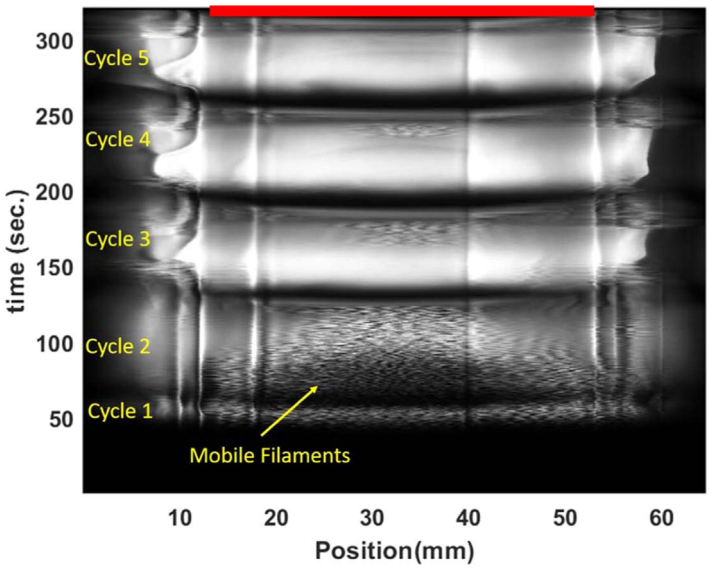

Fig. 6. (Color online) Space time evolution of particle growth (white scattered light in the image) at $B = 2$ T. The fluctuations in the middle region of the image (underneath the red bar) show the evidence of mobile filaments in the early growth cycles. The vertical strips near 10, 18, 40, and 55 mm show the locations of "locked" (i.e. spatially fixed) filaments. It is noted that with the later growth cycles (cycles 3–5), the nanoparticle density is very high and this is correlated to the suppression of the mobile filaments.

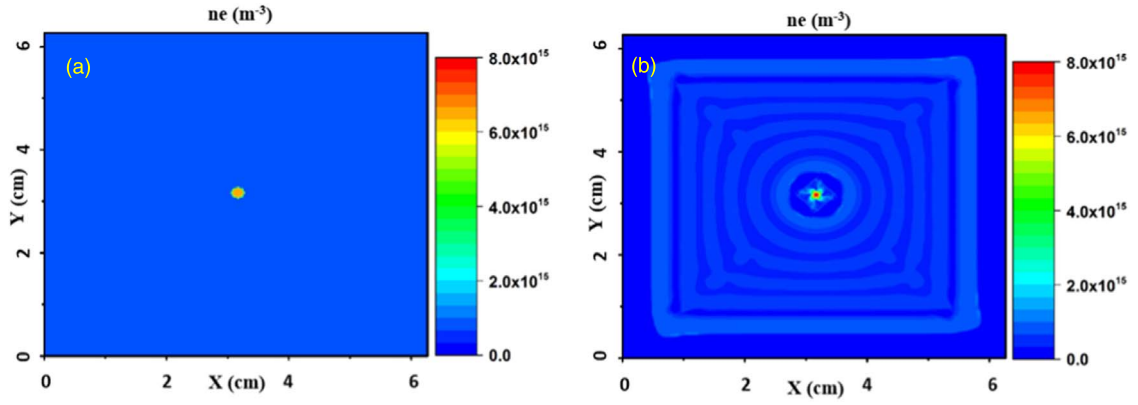

Fig. 7. (Color online) *x*–*y* cross-section of electron density profile in the middle of the argon plasma at pressure of 20 pa exposed to 2 T magnetic field in a rectangular chamber with fully conducting walls. (a) Initial condition, (b) at $t = 30\ \mu$s.

$$q_\alpha n_\alpha (\boldsymbol{E} + \boldsymbol{V_\alpha} \times \boldsymbol{B}) - k_B T_\alpha \nabla \boldsymbol{n_\alpha} - m_\alpha n_\alpha \upsilon_\alpha \boldsymbol{V_\alpha} = m_\alpha n_\alpha \frac{d\boldsymbol{V_\alpha}}{dt}, \quad (2)$$

where q_α is the electron/ion charge, n_α the electron/ion density, **E** the electric field vector, k_B the Boltzmann's constant, T_α the electron/ion temperature, m_α is the electron/ion mass, υ_α the electron/ion collision frequency with neutral atoms and $\boldsymbol{V_\alpha}$ is the velocity vector.

For constant electron/ion temperatures ($T_e = 2$ eV and $T_i = 0.025$ eV) you can refer to[17–21)]

The flux of each species, $\boldsymbol{\Gamma_\alpha}$:

$$\boldsymbol{\Gamma_\alpha} = n_\alpha \boldsymbol{V_\alpha}, \quad (3)$$

$$\frac{\partial n_\alpha}{\partial t} + \nabla \cdot \boldsymbol{\Gamma}\alpha = \sigma_I - \sigma_L \quad (4)$$

in which σ_I and σ_L are the ionization and recombination rates, respectively. For the whole set of chosen equation you can refer to.[22–30)]

In order to break the symmetry of the background plasma and excite the filamentary patterns, a high density column of electron and ion is introduced to the center of the plasma. It is noted that the time required for the evolution of filamentary patterns is shorter if a larger perturbation is introduced into the plasma bulk so we assumed the perturbation column to have a density of 5×10^{15} m^{-3} (i.e. a factor of 10 above the background plasma density). It takes about 20–30 μs for the patterns to form in the plasma as it was also noted by Menati et al.[15)] Additionally, in all simulations, the neutral gas pressure is assumed to be 20 pa and the magnetic field strength to be 2 T and we have simulated an argon plasma in a 6 cm × 6 cm × 4 cm chamber.

The simulation is first performed with the assumption that all of the chamber walls are fully conducting and there is no dust layer (or dielectric plate) in the plasma. Therefore, because of these perfectly conducting walls, any electron or ion that makes it to the walls is fully absorbed by the walls. The *x*–y cross-section of electron density profile in the middle of the chamber is depicted in Fig. 7(b) along with initial condition of the simulation [Fig. 7(a)]. The ion density profile and plasma potential are following exact same patterns as the electron density profile so they are not displayed here. As it can be seen in this figure the patterns are circular in the middle of the chamber but are rectangular near the walls due to the rectangular geometry of the walls.

It has to be noted that due to the fact that dust particles are much heavier than ions and they also carry charges much higher than electron and ions, the time-scale for the motion of the dust particles is in the order of few seconds while the dynamic of electrons and ions is in the order of micro-second to nano-second. Therefore, it is not currently practical to simulate a dusty plasma including the background plasma and heavy dust particles. Consequently, to simulate the presence of high density dust layers at the bottom of the chamber, we allow electrons and ions to accumulate in up to 5 layers near the bottom electrode and do not have them absorbed by the bottom electrode. Also, we are not allowing any charge transfer from one simulation cell to another. The outcome of this simulation is displayed in Fig. 8. As it can be noted in this figure, letting the charged particles to accumulate in few layers at the bottom of the chamber and considering zero conductivity for those layers, results in preventing the patterns to form in the plasma. This simulation proves again that the surface interaction of the dust particles with electrodes plays an important role in filamentation and pattern formation in magnetized plasmas.

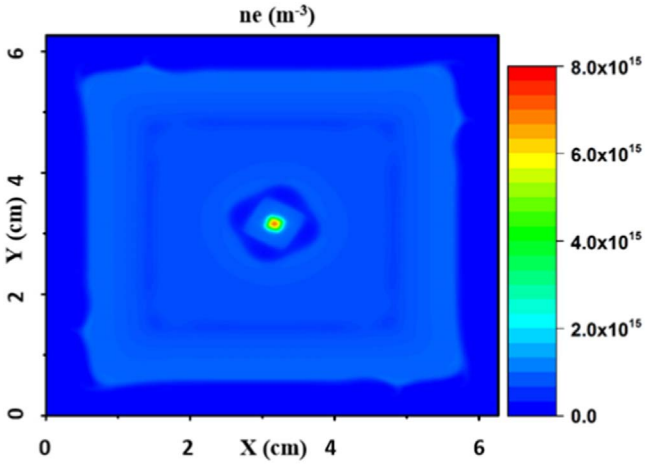

Fig. 8. (Color online) *x*–*y* cross-section of electron density profile in the middle of the argon plasma at pressure of 20 pa exposed to 2 T magnetic field at $t = 30\ \mu$s in a rectangular chamber by allowing electrons/ions to accumulate at the bottom of the chamber to simulate the presence of high density dust layers.

From the results above, it has been found that the filaments depends on the conductivity of the electrodes and an increasing number density of dusts near the lower electrode or replacing the metal electrodes with dielectric ones would suppress the filamentation. It is thought that the flux of the charged particles parallel to the external magnetic field has an important role in the quality of the filamentation. Therefore, by increasing the density of dust particles in the plasma chamber and their accumulation near the bottom electrode interferes with the effective flux of current channels to the bottom electrode which results in suppression of the filamentation.

6. Conclusions

In conclusion, we present an experimental investigation on the influence of nanoparticle growth on the magnetic field induced filaments. Experiments were performed in pure argon and argon acetylene plasmas at magnetic fields up to $B = 2.0\,\mathrm{T}$. It was found that high magnetic field strength has a major effect on the plasma glow distribution. To understand the effect of high density particles on the plasma a numerical model has been developed. The model confirmed that the higher density of nanoparticle growth help suppressing the filamentary structure and qualitatively a good agreement was found between the model and the experimental observations of the suppression of the filaments.

Acknowledgments

This material is based upon work supported by the U.S. Department of Energy, Office of Science, Office of Fusion Energy Sciences under award number DE-SC-0019176. This research used resources of the Magnetized Plasma Research Laboratory (MPRL) at Auburn University, which is a collaborative research facility supported by the U.S. Department of Energy, Office of Science, Office of Fusion Energy Sciences. Additional support is provided the National Science Foundation EPSCoR program (OIA-1655280), including funding for co-authors (S.J., M.M., V.H. H., V. R, and E. T.). The MDPX facility was developed and built through a grant from the NSF Major Research Instrumentation (NSF-MRI) program: PHY-1126067.

ORCID iDs

S. Jaiswal https://orcid.org/0000-0002-8447-2739

1) P. R. I. Cabarrocas, T. Nguyen-Tran, Y. Djeridane, A. Abramov, E. Johnson, and G. Patriarche, J. Phys. D: Appl. Phys. **40**, 2258 (2007).
2) U. R. Kortshagen, R. M. Sankaran, R. N. Pereira, S. L. Girshick, J. J. Wu, and E. S. Aydil, Chem. Rev. **116**, 11061 (2016).
3) M. Calafat, D. Escaich, R. Clergereaux, P. Raynaud, and Y. Segui, Appl. Phys. Lett. **91**, 181502 (2007).
4) N. Nafarizal and K. Sasaki, J. Phys. D: Appl. Phys. **45**, 505202 (2012).
5) A. Drenik, P. Yuryev, A. Vesel, J. Margot, and R. Clergereaux, Phys. Plasmas **20**, 100701 (2013).
6) K. Matyash, M. Fröhlich, H. Kersten, G. Thieme, R. Schneider, M. Hannemann, and R. Hippler, J. Phys. D: Appl. Phys. **37**, 2703 (2004).
7) L. Couëdel et al., Plasma Res. Express **1**, 015012 (2019).
8) M. Schwabe, U. Konopka, P. Bandyopadhyay, and G. E. Morfill, Phys. Rev. Lett. **106**, 215004 (2011).
9) P. Bandyopadhyay, D. Sharma, U. Konopka, and G. Morfill, AIP Conf. Proc. **1582**, 281 (2014).
10) E. Thomas, U. Konopka, R. L. Merlino, and M. Rosenberg, Phys. Plasmas **23**, 055701 (2016).
11) E. Thomas Jr. et al., Plasma Phys. Control. Fusion **62**, 014006 (2020).
12) E. Thomas Jr, R. L. Merlino, and M. Rosenberg, Plasma Phys. Control. Fusion **54**, 124034 (2012).
13) E. Thomas et al., J. Plasma Phys. **80**, 803 (2014).
14) E. Thomas, U. Konopka, B. Lynch, S. Adams, S. LeBlanc, R. L. Merlino, and M. Rosenberg, Phys. Plasmas **22**, 113708 (2015).
15) M. Menati, E. Thomas, and M. J. Kushner, Phys. Plasmas **26**, 063515 (2019).
16) S. K. Park and D. J. Economou, J. Appl. Phys. **68**, 3904 (1990).
17) S. Nunomura et al., J. Appl. Phys. **36**, 877 (1997).
18) Y. Tomita et al., Plasma Sci. Technol **7**, 2657 (2005).
19) N. Sternber, V. Godyak, and D. Hoffman, Phys. Plasmas **13**, 063511 (2006).
20) A. R. Niknam, T. Haghtalab, and S. M. Khorashadizadeh, Phys. Plasmas **18**, 113707 (2011).
21) J. González and L. Conde, Phys. Plasmas **26**, 043505 (2019).
22) D. B. Graves and K. F. Jensen, IEEE Trans. Plasma Sci. **14**, 78 (1986).
23) Y.-H. Oh, N.-H. Choi, and D.-I. Choi, J. Appl. Phys. **67**, 3264 (1990).
24) M. H. Wilcoxson and V. I. Manousiouthakis, IEEE Trans. Plasma Sci. **21**, 213 (1993).
25) A. Bogaerts, R. Gijbels, and W. J. Goedheer, J. Appl. Phys. **78**, 2233 (1995).
26) H. Akashi, Y. Sakai, N. Takahashi, and T. Sasaki, J. Phys. D **32**, 2861 (1999).
27) S. Medina, K. Yanallah, L. Mehdaoui, A. Belasri, and T. Baba-Hamed, Plasma Devices Oper. **13**, 1 (2005).
28) A. Derzsi, P. Hartmann, I. Korolov, J. Karácsony, G. Bánó, and Z. Donkó, J. Phys. D: Appl. Phys. **42**, 225204 (2009).
29) Q. Liu, Y. Liu, and Z. Ma, Phys. Plasmas **21**, 083511 (2014).
30) S. I. Eliseev, E. A. Bogdanov, and A. A. Kudryavtsev, Phys. Plasmas **24**, 093503 (2017).